High-Efficiency Carrier Multiplication and Ultrafast Charge Separation in Semiconductor Nanocrystals Studied via Time-Resolved Photoluminescence†

Richard D. Schaller,* Milan Sykora, Sohee Jeong, and Victor I. Klimov*

Chemistry Division, MS-J567, Los Alamos National Lab, Los Alamos, New Mexico 87545

Received: August 15, 2006; In Final Form: August 31, 2006

We demonstrate novel methods for the study of multiple exciton generation from a single photon absorption event (carrier multiplication) in semiconductor nanocrystals (or nanocrystal quantum dots) that are complementary to our previously reported transient absorption method. By monitoring the time dependence of photoluminescence (PL) from CdSe nanocrystals via time-correlated single photon counting, we find that carrier multiplication is observable due to the Auger decay of biexcitons. We compare these data with similar studies using transient absorption and find that the two methods give comparable results. In addition to the observation of dynamical signatures of carrier multiplication due to the Auger decay, we observe spectral signatures of multiple excitons produced from the absorption of a single photon. PL spectra at short times following excitation with high-energy photons are red-shifted compared to the single-exciton emission band, which is consistent with previous observations of significant exciton−exciton interactions in nanocrystals. We then show using a combination of transient absorption and time-resolved PL studies that charge transfer between a nanocrystal and a Ru-based catalyst model compound takes place on a time scale that is faster than Auger recombination time constants, which points toward a possible design of donor−acceptor assemblies that can be utilized to take advantage of the carrier multiplication process.

1. Introduction

Generation of multiple electron−hole pairs (excitons) following the absorption of a single high-energy photon is a process that can potentially improve the performance of many semiconductor-based devices such as solar cells, photocatalysts (for, e.g., generating solar fuels), photodetectors, optical amplifiers, etc. This effect, which is generally referred to as carrier multiplication (CM), can improve device efficiency because of creation of a larger number of excitons for the same number of absorbed photons.

In terms of the quantum efficiency (QE) with which an absorbed photon produces excitons in a semiconductor, CM makes it possible for the QE to exceed 100% for sufficient values of $\hbar\omega_p/E_g$ ($\hbar\omega_p$ is the photon energy and E_g is the semiconductor energy gap), whereas QE is always 100% in the absence of CM for $\hbar\omega_p/E_g \geq 1$. Although CM has been known to take place in bulk semiconductors since 1957,[1] it does not occur with significant efficiency in the range of solar photon energies (0.5−3.5 eV). The potential benefits of CM have been discussed extensively,[2−6] but the low CM efficiencies in bulk phase semiconductors and the lack of a means to reliably detect CM have caused the consideration of the process to be largely hypothetical in character. In 2004, however, we presented evidence using a novel transient absorption (TA) method that CM takes place with very high efficiency in PbSe semiconductor nanocrystals (NCs).[7] More recently we have demonstrated that this process also occurs in CdSe NCs,[8] which points toward the generality of this phenomenon to nanocrystalline materials. Furthermore, using PbSe NCs we have shown that as many as seven excitons can be generated from a single photon of sufficient energy, which corresponds to the ultimate limit defined by energy conservation.[9,10] Recently, Nozik's group has also implemented this dynamic TA technique in similar studies of CM in PbSe NCs as well as in NCs of PbS[11] and PbTe.[12]

The TA method for detecting CM and quantifying its efficiency is based on a significant difference in recombination dynamics of single excitons and multiexcitons. Specifically, in well-passivated NCs, single excitons decay primarily via relatively slow radiative recombination, which is characterized by tens (CdSe NCs)[13] to hundreds (PbSe NCs)[14,15] of nanosecond time scales. In contrast, if more than one exciton is generated per NC, then the recombination dynamics are dominated by nonradiative Auger recombination, which occurs on much shorter tens to hundreds of picosecond time scales.[16,17] Thus, femtosecond TA is well-suited for detecting the difference in recombination dynamics of single excitons and multiple excitons.

In TA measurements, a femtosecond laser system is used to produce pump and probe laser pulses, each of which is preferably tunable. The probe pulse is tuned to the energy of the lowest-energy excitonic absorption feature (the 1S exciton) in the NC sample, which approximately corresponds to E_g, and the pump pulse is tuned to values of $\geq E_g$. After excitation of the NC sample, the probe pulse is used to monitor exciton populations in the NCs as a function of time. At lower pump photon energies ($<2E_g$) and low pump intensity, a NC will absorb a single photon and produce a single exciton, which results in a bleach of the 1S feature that exists for a time related to the single-exciton radiative lifetime (in the absence of carrier trap sites). At higher pump intensity, two photons can be absorbed by the NC from the same pump pulse, which results in the formation of biexcitons and a correspondingly larger bleach signal. Once generated, though, biexcitons are able to undergo the rapid process of Auger recombination in which one

† Part of the special issue "Arthur J. Nozik Festschrift".

* Authors to whom correspondence should be addressed. E-mail: rdsx@lanl.gov; klimov@lanl.gov.

10.1021/jp065282p CCC: $33.50
Published on Web 10/31/2006

exciton recombines by depositing the recombination energy into either the electron or the hole of the other exciton, which leaves the NC with a single exciton at later times. Upon excitation of NCs with high pump photon energy at low intensity whereby a single photon is absorbed per NC, dynamics consistent with the Auger recombination of biexcitons have been observed, which indicates that CM occurs in NCs.[7] Because Auger recombination is significantly faster than radiative recombination,[16] the efficiency of CM can be determined from the ratio of bleaching at early times when multiple excitons exist in a NC versus later times when a single exciton remains for each NC that was photoexcited.[7] Studies of CM efficiency have shown that the process has a well-defined threshold and also exhibits a surprisingly linear dependence upon the ratio of $\hbar\omega_p$ to E_g.[8,10]

While TA has been used to successfully demonstrate CM in NCs, it is also the only reported technique to directly study it at this time. Additional techniques for the study of CM are needed to obtain more information about the process and also to extend these studies to materials for which TA is not a viable technique. For instance, materials that exhibit long multiexciton lifetimes are difficult to study with ultrafast TA due to practical considerations of physically delaying the probe pulse without affecting measurement accuracy. Furthermore, indirect-gap NC materials do not exhibit clear bleaching features due to saturation of quantized states but instead show broad-band photoinduced absorption that is not directly related to occupancy of quantized levels. Further, NC ionization following photoexcitation can also complicate interpretation of TA signals because TA features of charged NCs might be significantly different from those of the charge-neutral material. Finally, TA experiments normally require a relatively complex and expensive amplified laser system, suffer from laser intensity variations, and also are impaired because measurements of small signal changes are conducted with a large background.

Photoluminescence (PL) measurements offer a number of advantages in CM studies compared to TA measurements including, for example, higher sensitivity (potentially down to the single NC level), simplicity, and availability with regard to instrumentation. Here, we demonstrate for the first time that time-resolved PL is a viable method for detecting CM and measuring its efficiency. We perform side-by-side studies of CM in CdSe NCs using both time-resolved PL and TA and find that measured efficiencies of CM are comparable for the two techniques. In addition to the observation of CM via *dynamical* signatures, here we also demonstrate that *spectral* signatures of biexcitons are observable in time-resolved PL. Specifically, we show that early-time PL following excitation with a high-energy photon at low intensity produces the same spectral shift as is observed from the generation of biexcitons via absorption of multiple photons in CdSe NCs using high-intensity, low-photon-energy excitation. This finding reinforces that CM is indeed observed in both the time-resolved PL and TA methods as it rules out any other dynamical processes that by coincidence have matching rates with the Auger recombination of multiexcitons. We then perform studies of charge transfer between CdSe NCs and a model ruthenium-containing catalytic complex and show that hole transfer from the NC to the Ru complex takes place on a sufficiently fast time scale for taking advantage of the CM effect.

2. Experimental Section

In this work, we study high-quality, nearly spherical, colloidal CdSe NC samples that are fabricated via an organometallic route.[18] The NC mean radii are from 1.2 to 4.2 nm, and the size dispersion is from 5% to 9%, respectively. The CdSe NC surface was passivated with either trioctylphosphine oxide (TOPO) or a ZnS shell followed by TOPO. Samples were dispersed in hexane except where noted. To monitor carrier population dynamics, we use a time-resolved PL experiment in which NCs are excited by 100 fs pulses that are derived from a 250 kHz amplified Ti:sapphire laser with a photon energy of either 3.1 or 6.2 eV. PL lifetimes are measured using a multichannel plate detector and time-correlated single photon counting (TCSPC) electronics. The width of the instrument response function (mainly determined by the detector) is ~45 ps. TA data are collected using a 50 fs pulse width, 1 kHz amplified Ti:sapphire laser that is used to pump two independently tunable optical parametric amplifiers.[7] In TA studies the probe pulse is tuned to the position of the 1S exciton absorption feature. All measurements are performed at room temperature.

3. Results and Discussion

3.1. Determination of CM Efficiencies Using TA and PL Dynamics. First, we show that both TA and time-resolved PL measurements can be used to detect and measure CM efficiency *dynamically*. Below, we consider the situation for which the QE is less than 200% following single photon absorption (which is the case in the experiments discussed below), and hence, photoexcitation only produces either single excitons or biexcitons. First, for photoexcitation that does not result in CM, the bleach of the lowest-energy 1S exciton state in CdSe NCs ($\Delta\alpha_{1S}$) measured in TA experiments is simply proportional to the average number of excitons produced per NC, $\langle N\rangle$, $|\Delta\alpha_{1S}|/\alpha_{0,1S} = \langle N\rangle/2$, where $\alpha_{0,1S}$ is the 1S ground-state absorption.[19] Also, immediately after photoexcitation $\langle N\rangle = j_p\sigma_a$ where j_p is the pump pulse fluence and σ_a is the NC absorption cross-section. Interestingly, time-resolved PL exhibits a similar dependence on $\langle N\rangle$. Instantaneous PL intensity (I_{PL}) is proportional to the ratio of a density of emitters and the emitter radiative lifetime. In the case of a NC ensemble that only contains excitons and biexcitons, it can be presented as $I_{PL} \propto n_1/\tau_{r,1} + n_2/\tau_{r,2}$, where n_1 and n_2 are the fractions of singly and doubly occupied NCs in the ensemble, respectively, and $\tau_{r,1}$ and $\tau_{r,2}$ are corresponding radiative lifetimes. Since $\tau_{r,2} = \tau_{r,1}/2$, the expression for I_{PL} can be rewritten as follows: $I_{PL} \propto (n_1 + 2n_2)/\tau_{r,1} = \langle N\rangle/\tau_{r,1}$, indicating the same type of proportionality with respect to $\langle N\rangle$ as in the case of TA signals measured for the 1S exciton.

A convenient characteristic of a photoexcited ensemble in CM studies is the average exciton multiplicity, $\langle N_x\rangle$, which is defined as the average number of excitons per photoexcited NC.[9] This quantity relates to $\langle N\rangle$ by $\langle N_x\rangle = \langle N\rangle/n_x$, where $n_x = n_1 + n_2$ is the fraction of NCs in the sample occupied with excitons independent of their multiplicity. We can further present both TA and PL signals in terms of $\langle N_x\rangle$ as $|\Delta\alpha_{1S}| \propto \langle N_x\rangle n_x$ and $I_{PL} \propto \langle N_x\rangle n_x$. In our dynamic method for quantifying the CM efficiency, we analyze the evolution of TA and PL signals on time scales that are longer than the Auger recombination time constants ($\tau_{A,2}$, $\tau_{A,3}$, ... for biexcitons, triexcitons, etc.) but shorter than the characteristic radiative lifetimes. On these time scales, n_x is constant (Auger recombination does not change the number of occupied NCs), and hence, TA and PL dynamics provide direct information on temporal changes in the average exciton multiplicity. Furthermore, since at the end of the Auger decay process $\langle N_x\rangle = 1$ (no multiexcitons remain in the system), the amplitude of the slow single-exciton component of the TA or PL signal at times $t > \tau_{A,2}$ (referred to as *b* in Figure 1) provides

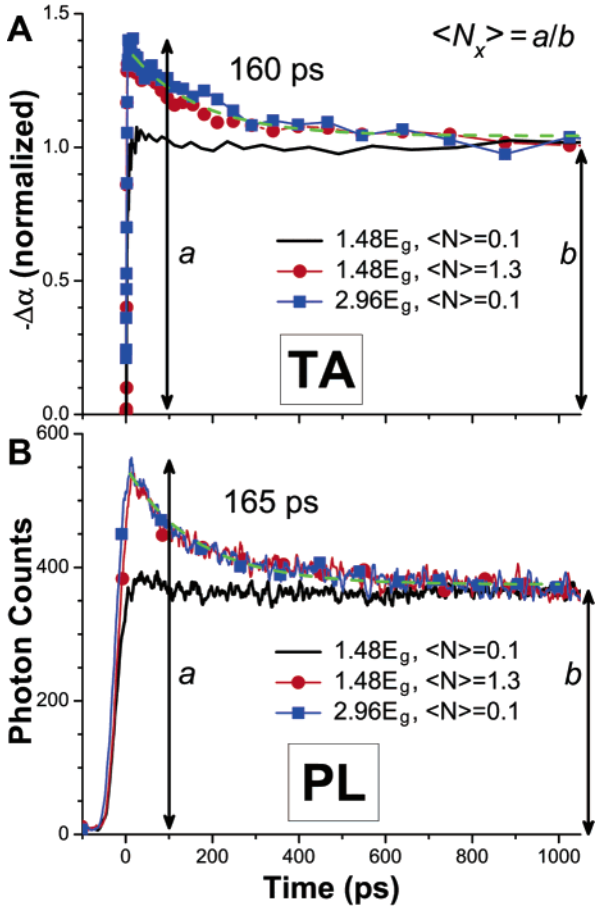

Figure 1. Dynamic measurements (all traces normalized at long time) of CM in TOPO-capped CdSe NCs (E_g = 2.09 eV) using (A) TA probed at the 1S exciton absorption feature and (B) time-resolved PL monitored at the steady-state emission maximum. The same sample of NCs was excited in three different ways: 3.1 eV photon energy at low intensity ($\langle N\rangle = 0.1$) such that single-exciton dynamics are observed (black line), 3.1 eV photon energy at higher intensity ($\langle N\rangle = 1.3$) such that more than one photon is absorbed per NC on average from a laser shot and biexciton dynamics are observed (red circles), and 6.2 eV photon energy at low intensity ($\langle N\rangle = 0.1$) such that less than one photon is absorbed per NC on average yet biexciton dynamics are observed due to CM (blue squares). Both TA and time-resolved PL produce very similar dynamic responses for each method of excitation. Observed relaxation dynamics of biexcitons generated either via absorption of multiple photons or via CM give a relaxation time constant of ~160 ps (experimental fits are shown by green dashed lines) that is due to nonradiative Auger recombination. The ratio of early-time amplitude to late-time amplitude following excitation with a 6.2 eV photon indicates the initial average multiplicity, $\langle N_x\rangle$ (i.e., CM efficiency in the case of excitation with high-energy photons).

a convenient scale bar for quantifying the exciton multiplicity (and hence the CM efficiency) immediately after photoexcitation, $\langle N_x\rangle = a/b$, where a is the amplitude of the TA or PL signal at short times after excitation ($t \ll \tau_{A,2}$) (Figure 1). The QE relates to $\langle N_x\rangle$ by QE = 100%$\langle N_x\rangle$.

In Figure 1A, we present TA measurements that we have previously shown reveal the generation of multiple excitons from the absorption of a single pump photon of sufficient energy.[7,8] TA time traces, which are normalized at long time delay, were produced under three different excitation conditions. First a TA time trace was collected using low-intensity ($\langle N\rangle = 0.1$) and low-photon-energy (3.1 eV) excitation (black line in Figure 1A) for which CM is not energetically possible (3.1 eV corresponds to only 1.48E_g). In this case, a long-lived bleach signal is observed, which is typical of a single exciton contained within each excited NC. Next, a TA time trace was collected using 3.1 eV photons at a higher intensity ($\langle N\rangle = 1.3$), and faster relaxation dynamics are observed at early times (red circles in Figure 1A). This fast dynamical component to the relaxation results from Auger recombination of biexcitons in NCs that form due to the absorption of multiple photons.[7,8,19] Finally, the sample is excited using higher photon energy (6.2 eV) at low intensity ($\langle N\rangle = 0.1$) (blue squares in Figure 1A). Under this condition, only single photons are absorbed by each NC that is excited; however, there is theoretically enough energy in each photon for a biexciton to be produced via CM (6.2 eV corresponds to 2.95E_g for this sample). In the TA time trace collected under these conditions, a fast relaxation component to the dynamics is in fact observed, which exhibits a decay that matches that produced using 3.1 eV photons at high intensity. This analysis indicates that multiple excitons can be efficiently produced from single photons of sufficient energy as we have reported in more detail previously.[7−10]

Next, time-resolved PL measurements, collected at the steady-state PL spectral maximum, were performed under the same three excitation conditions described above and are shown in Figure 1B (normalized at long times). Excitation of the sample using low-intensity ($\langle N\rangle = 0.1$) 3.1 eV photons produces long-lived dynamics in PL (black line in Figure 1B) due to generation of single excitons per excited NC, while higher pump intensity ($\langle N\rangle = 1.3$) at this energy produces a fast relaxation component at early times (red circles in Figure 1B). This fast relaxation component is similar to that observed in the TA measurement and has previously been attributed to the Auger recombination of biexcitons in time-resolved PL studies.[20] Finally, the sample was excited using low-intensity ($\langle N\rangle = 0.1$) 6.2 eV photons (blue squares in Figure 1B), and a fast relaxation component is observed at early delay, which has a relaxation time constant that is similar to that of biexcitons measured using the absorption of multiple photons. This measurement indicates that CM is indeed observable in time-resolved PL dynamics. Furthermore, these PL and TA studies show that similar dynamical information can be obtained for CdSe NCs using either method.

3.2. Quantitative PL Studies of CM Efficiency in the Presence of Fast Trapping. A potentially significant complication with the use of the time-resolved PL method became apparent during the course of these CM studies of many samples. Specifically, for some NC samples, single-exciton PL dynamics exhibit a fast relaxation component that is commonly observed for CdSe NCs of any radius when capped with TOPO and is also observed for large radius CdSe NCs overcoated with a wide band gap semiconductor (ZnS). Because these same samples do not exhibit a fast relaxation component for single-exciton dynamics measured using TA, the problem can be attributed to hole trapping.[21,22] In studies of II−VI NCs, 1S TA signals are dominated by electron dynamics because the energy spectra of the hole states are dense whereas those of the electron states are sparse. As a result, single-state occupation numbers for electrons are much greater than those for holes. (TA signals are proportional to the sum of these occupation numbers.) Time-resolved PL, however, is sensitive to the dynamics of either carrier since both must be present within a NC for electron−hole recombination to take place. (PL intensity is proportional to the product of the electron and hole occupation numbers.) Whereas this difference in carrier dynamic sensitivity can be exploited in, e.g., charge-transfer studies (see section 3.5), this fast relaxation component may complicate studies of CM using the time-resolved PL method. However, as indicated in the analysis below, time-resolved PL can still be used for quantify-

ing the CM efficiency even in the case of samples that show fast single-exciton dynamics due to efficient trapping.

In our analysis, we classify photoexcited NCs based on their relaxation dynamics into two subensembles of "short-lived" and "long-lived" NCs with relative fractions n_{xs} and n_{xl}, respectively, that relate to the total fraction of photoexcited NCs by $n_x = n_{xs} + n_{xl}$. We define long-lived NCs as those in which single-exciton relaxation dynamics are slower than biexciton Auger decay. This subensemble comprises NCs in which carrier relaxation is due to radiative decay and slow trapping (typical in CdSe NCs, e.g., for electron traps). Single-exciton dynamics in short-lived NCs are faster than those of the Auger decay, which is usually observed for hole trapping in CdSe NCs. We further assume that CM is faster than any of the trapping processes. On the basis of our recent results,[23] CM occurs on a sub-200-fs time scale; therefore, the latter condition is likely satisfied for most of the NC samples.

At low pump intensities and without CM, the PL intensity immediately after excitation is proportional to $n_x = n_{xs} + n_{xl}$ (signal amplitude a_0 in Figure 2A, black dashed line), while the PL intensity becomes proportional to n_{xl} after fast relaxation is finished and PL exhibits a long-lived plateau (signal amplitude b_0 in Figure 2A, black dashed line). Using amplitudes a_0 and b_0, we can calculate the relative fraction of NCs that exhibit slow relaxation behavior in the sample under investigation: $r_l = n_{xl}(n_{xs} + n_{xl})^{-1} = b_0/a_0$.

In the circumstance that CM takes place, which produces exciton multiplicity $\langle N_x \rangle$, the initial PL signal amplitude (a in Figure 2A, blue solid line) is proportional to $\langle N_x \rangle n_x = \langle N_x \rangle (n_{xs} + n_{xl})$ (see previous section) because it is assumed that CM is faster than any recombination/trapping process in the material. However, the signal at long times (longer than the Auger decay time) is still proportional to n_{xl} (as in the no-CM case) (signal amplitude b in Figure 2A, blue solid line), because in short-lived NCs all carriers rapidly relax via a combined effect of Auger recombination and fast trapping, while in long-lived NCs Auger recombination reduces the exciton multiplicity to 1. On the basis of these considerations we obtain that the ratio of PL intensities at short and long times after excitation is $a/b = \langle N_x \rangle (n_{xs} + n_{xl}) n_{xl}^{-1} = \langle N_x \rangle r_l^{-1}$, which further indicates that the average exciton multiplicity can be calculated as $\langle N_x \rangle = (a/b) r_l = (a/b)(b_0/a_0)$. This expression provides a recipe for calculating the CM efficiency based on PL dynamics measured below and above the CM threshold. A simple practical approach for quantifying the CM efficiency is illustrated in Figure 2B where we show time-resolved PL data collected at low excitation intensity ($\langle N \rangle = 0.1$) with (blue solid line) and without CM (black dashed line) that have been normalized at long times. In this case, CM efficiency is related to the ratio of the maxima of the early-time instantaneous PL in the two traces ($\langle N_x \rangle = a/a_0$ if $b = b_0$). This same experimental method of determination of CM in the presence of fast trapping is viable in TA measurements.

3.3. Comparison of CM Efficiencies Measured Using PL and TA. Figure 3 shows the QE of exciton generation as a function of $\hbar\omega_p/E_g$ measured via TA[8] (black squares) as well as via time-resolved PL (red circles). Our previous TA work indicates that CdSe NCs exhibit a threshold for CM of approximately $2.5E_g$ above which we observe a linear increase of QE with a slope of $\sim 100\%/E_g$. The time-resolved PL data generally agree with this trend as there appears to be an onset for CM of $\sim 2.5E_g$, and although there is more scatter in the QE measurements taken from time-resolved PL, the QE increase is almost linear with $\hbar\omega_p/E_g$.

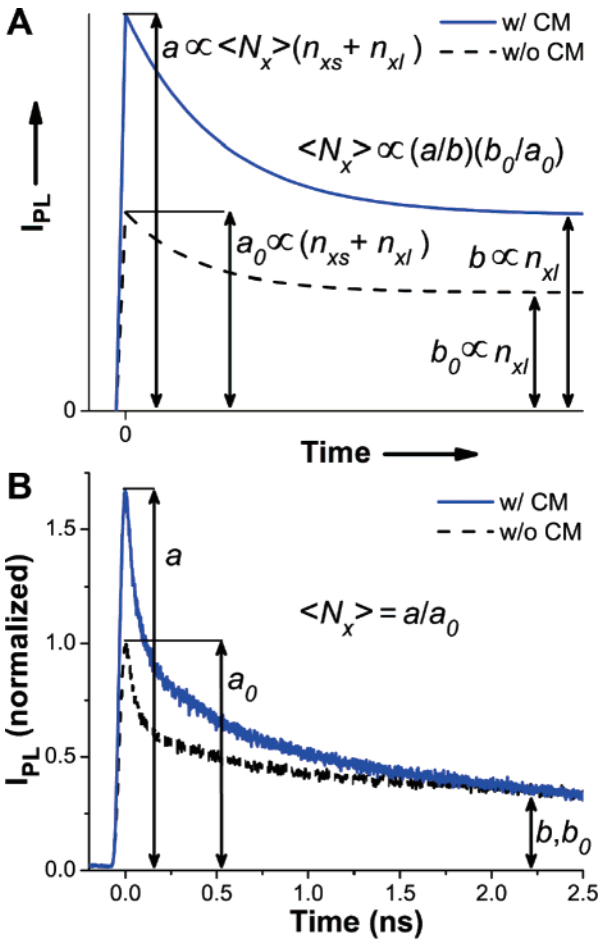

Figure 2. Determination of CM efficiency in materials that exhibit a fast relaxation component in single-exciton dynamics. (A) Ensemble single-exciton dynamics are produced from a fraction of photoexcited NCs that is short-lived (n_{xs}) and a fraction that is long-lived (n_{xl}). The instantaneous PL amplitude (a_0) just after excitation is proportional to $n_{xs} + n_{xl}$, and the amplitude at longer delays (but before τ_{rad}) (b_0) is proportional only to n_{xl} (black dashed line). Because CM takes place on a very fast time scale (before intraband relaxation), photoexcitation that results in CM will cause the maximum instantaneous PL amplitude (a) to be proportional to $\langle N_x \rangle (n_{xs} + n_{xl})$, but at longer delays the amplitude (b) will again be proportional to n_{xl} since Auger recombination is a very fast process in NCs (blue solid line). Thus, $\langle N_x \rangle$ can be determined from the ratio of the early-time amplitudes if the traces are normalized at long delays. (B) CM efficiency can be determined via time-resolved PL data (normalized at long times) for a CdSe NC sample ($E_g = 1.91$ eV) that exhibits significant carrier trapping using low-intensity excitation ($\langle N \rangle = 0.1$) with 3.1 eV (black dashed line) and 6.2 eV excitation (blue solid line).

Taken together, the dynamic PL and TA studies presented indicate that similar information regarding CM can be acquired using either technique. Thus, the general advantage of the PL method is that it is simpler to perform than TA as only a single tunable laser pulse is required and the low background levels associated with PL studies allows the use of very low pump intensity or low sample density while high signal-to-noise ratios can be maintained. However, the technique is more sensitive to carrier trapping than TA and is also limited by the availability of fast detectors in some spectral regions of interest. The time resolution of TCSPC is also not quite high enough to precisely determine Auger recombination times of biexcitons, whereas TA has very high temporal resolution. Other methods of measuring time-resolved PL do have time resolution that is equivalent to TA such as femtosecond PL upconversion,[24,25] which we are currently investigating.

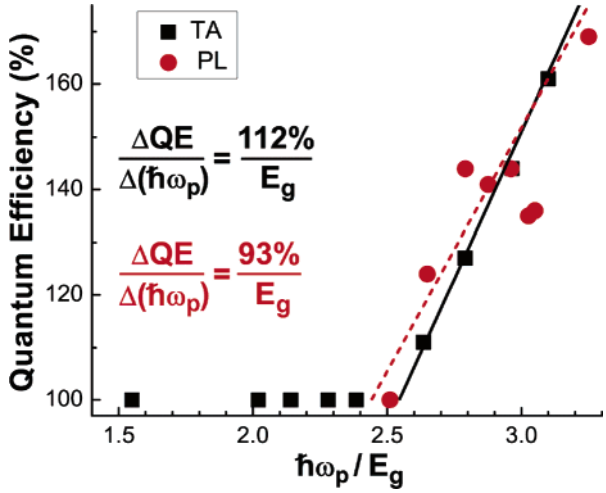

Figure 3. Quantum efficiency of photon-to-exciton conversion measured using TA (black squares) and time-resolved PL (red circles) as a function of $\hbar\omega_p/E_g$ for several CdSe NC samples. Both TA and time-resolved PL data exhibit a CM onset of $\sim 2.5E_g$ and a roughly linear increase of efficiency with $\hbar\omega_p/E_g$ ($\sim 100\%/E_g$) above that onset. Linear fits to the TA and PL data are shown by the black solid line and the red dashed line, respectively. Slopes of these fits ($\Delta QE/\Delta\hbar\omega$) are indicated in the figure.

It is also noteworthy that we have not noted any difference in CM efficiency for CdSe NCs that have a thin inorganic shell of ZnS rather than an organic-based surface passivating layer using either TA or time-resolved PL. The only noticeable difference is the expected increase in absorption cross-section for the core−shell NC material at photon energies that are absorbed by the shell layer.

3.4. Spectral Signatures of Biexcitons Produced by CM. Next, time-resolved PL experiments were performed that demonstrate for the first time that CM can also be detected via the *spectral* signatures of biexcitons in addition to their dynamic signatures. In CdSe NCs, biexcitons exhibit exciton−exciton interaction energies, Δ_{XX}, which are enhanced (up to more than 30 meV)[20,26] relative to the bulk (4.5 meV).[27] The interaction between two excitons within a spherical NC is attractive and causes the emission of a biexciton to be red-shifted relative to that of a single exciton in a NC (Figure 4A). Because Auger recombination causes the lifetimes of biexcitons to be much shorter than their radiative lifetimes, emission from such states is only observable when it is time-resolved. Time-resolved PL spectra were measured using two different excitation conditions that produce biexcitons and are shown in Figure 4B. First, spectra were collected using 3.1 eV photon energy with $\langle N\rangle = 2.5$. Upon arrival of the excitation pulse (nominally time zero with our 40−50 ps resolution), PL spectra exhibit a red-shifted emission maximum (red circles) in comparison to spectra measured at later times (black line). At long temporal delays, after nonradiative Auger recombination of biexcitons has taken place (>500 ps for this sample), only single excitons remain in the population of excited NCs, which causes measured spectra to be identical to the time-integrated PL spectrum of the sample. The spectral component extracted from the difference of the spectra measured immediately after excitation and at long times following the pump pulse can be fit with a Gaussian profile and exhibits a red shift of tens of meV, which is consistent with previous measurements of Δ_{XX} for CdSe NCs.[20]

Time-resolved PL spectra were then measured using low-intensity ($\langle N\rangle = 0.001$) 6.2 eV photons (Figure 4B) for which CM is possible. Again it can be seen that spectra collected immediately after arrival of the excitation pulse exhibit a red-shifted PL maximum at early times (blue squares). A Gaussian fit of the difference of early and later time PL spectra exhibits roughly the same shift that is observed using absorption of multiple photons to produce biexcitons. This red-shifted spectral feature that is observed at early times is indicative of the generation of biexcitons from single photons. Thus, this study shows that spectroscopic methods, in addition to our dynamic method (shown above), are viable means for the study of CM.

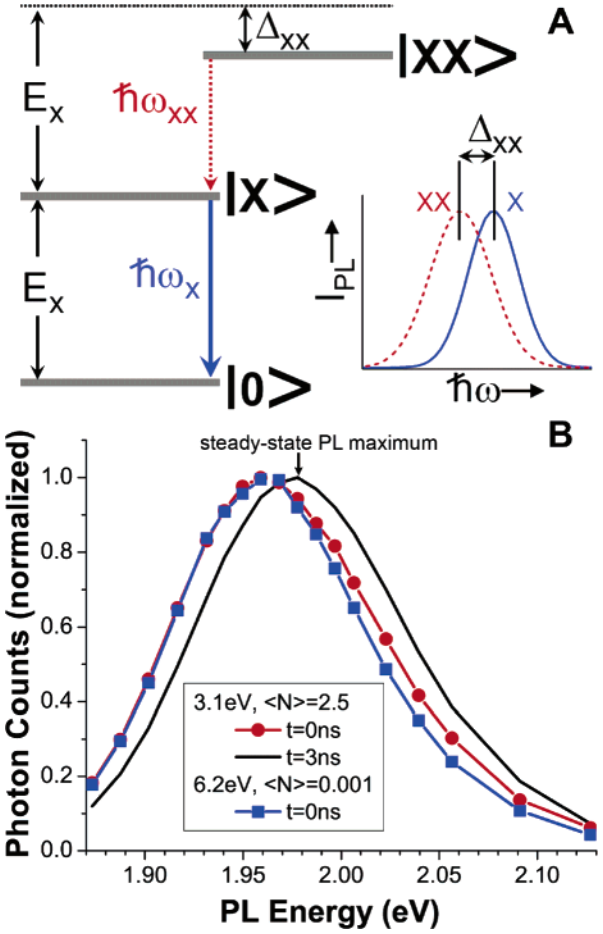

Figure 4. Spectral method of observation of CM in NCs. (A) A single exciton in a NC will emit a photon of energy $\hbar\omega_x$ upon electron−hole recombination. However, if the same NC contains a biexciton, then the emitted photon energy, $\hbar\omega_{XX}$, is decreased by an exciton−exciton interaction energy, Δ_{XX}. These two different emission wavelengths (each of which has a spectral bandwidth that is largely determined by the size dispersity of the NC ensemble) will convolute early time delay spectra to lower energy until nonradiative Auger recombination removes biexcitons from the NC. (B) A sample of CdSe NCs ($E_g = 1.98$ eV) was excited with 3.1 eV photons at a high enough intensity to produce biexcitons in a majority of the NCs ($\langle N\rangle = 2.5$). The PL spectrum measured at zero delay from the excitation pulse (red circles) is clearly red-shifted with respect to the spectrum measured at a delay of 3 ns (black line) when only single excitons remain. This long delay spectrum is identical to the steady-state PL spectrum. Excitation with 6.2 eV photons at a very low intensity ($\langle N\rangle = 0.001$) such that NCs only absorb a single photon per each laser shot also exhibit the same red-shifted PL spectrum at zero delay from the excitation pulse (blue squares).

3.5. Charge Extraction from NCs Using NC/Ru Complex Assemblies. For the CM effect to be utilized in practical applications, carriers need to be extracted from NCs on time scales that are shorter than the characteristic Auger recombination times of multiexcitons. Achievement of this goal depends on a good understanding of the mechanism and dynamics of the charge-transfer processes occurring at the surface of the NCs.[28−32] Time-resolved PL and TA techniques are powerful

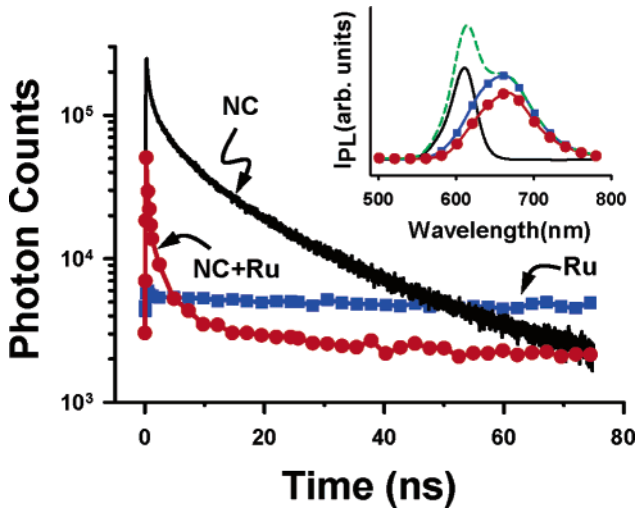

Figure 5. Time-resolved PL of CdSe NCs (black line), $[Ru(bpy)(mcb)_2]^{2+}$ (blue squares), and the NC/$[Ru(bpy)(mcb)_2]^{2+}$ assembly (red circles) measured in benzonitrile using TCSPC. The concentrations of the NCs and Ru complex in the assembly were identical to the concentrations of NCs and Ru complex in the reference samples. The excitation and monitoring wavelengths were 402 and 610 nm, respectively, and $\langle N \rangle = 0.001$. The inset shows the steady-state PL spectra of the same samples measured in benzonitrile. The dashed green line is a numerical sum of the spectra of the CdSe NCs (black line) and $[Ru(bpy)(mcb)_2]^{2+}$ (blue squares).

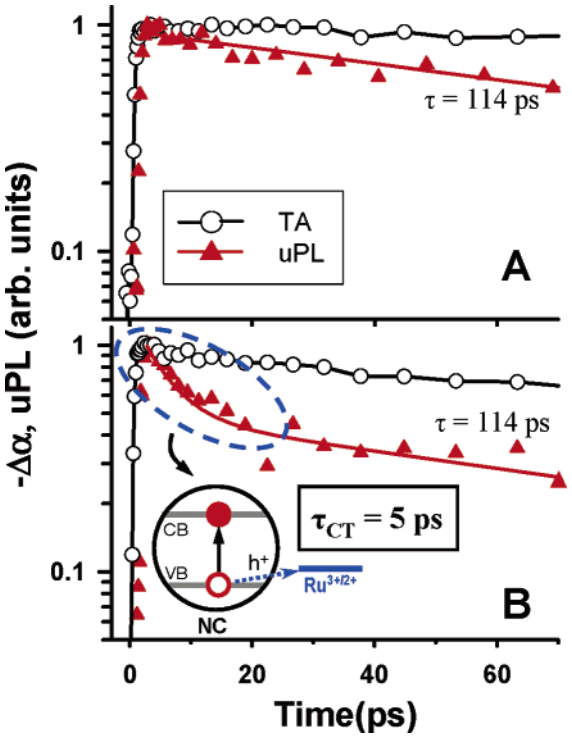

Figure 6. (A) Comparison of the TA (circles) and uPL (triangles) dynamics measured for the CdSe NCs and (B) the NC/$[Ru(bpy)(mcb)_2]^{2+}$ assembly. The TA and PL signals were collected at 600 and 615 nm, respectively. The excitation wavelength was 400 nm, and $\langle N \rangle = 0.2$. The inset shows the mechanism of the charge-transfer process between the CdSe NCs and the surface-adsorbed $[Ru(bpy)(mcb)_2]^{2+}$, which is shown to occur with a 5 ps time constant; this time corresponds to the interaction of a single NC with multiple surface-adsorbed Ru complexes.

tools for the study of these processes. Figures 5 and 6 show an example where the combination of PL and TA is used to elucidate the mechanism and dynamics of charge transfer between TOPO-capped CdSe NCs and a surface-adsorbed transition metal complex $[Ru^{II}(bpy)(mcb)_2]^{2+}$ (where bpy = 2,2′-bipyridine and mcb = 4-carboxy-4′-methyl-2,2′-bipyridine). The results of these studies indicate the feasibility of ultrafast extraction of holes from NCs that can compete with the Auger decay.

Figure 5 shows time-resolved PL traces of CdSe NCs (with a 2.3 nm mean radius) in benzonitrile solution in the absence (black line) and in the presence (red circles) of surface-adsorbed Ru complexes measured using TCSPC. The time-resolved PL of the Ru complex (blue squares) is included for comparison. All traces are recorded at 610 nm, which corresponds to the NC PL maximum. The inset shows the steady-state PL spectra for the same samples (with the symbols and coloring scheme the same as in the main frame). The steady-state spectrum of the NC/Ru complex assembly does not indicate any detectable NC PL, while it is clearly visible in the emission spectrum of the reference NC sample with the same NC concentration (NC PL emission peak $\lambda_{NC}^{max} = 610$ nm). The PL of the Ru complex ($\lambda_{Ru}^{max} = 670$ nm) is also partially quenched in the assembly, which is evident from the comparison with the PL spectrum of the Ru complex reference (the ratio of emission intensities $I_{PL}(NC/Ru)/I_{PL}(Ru) \approx 0.6$ at 610 nm).

Because of spectral overlap of the NC and the Ru complex emission bands, time-resolved PL of the NC/Ru complex assembly monitored at 610 nm has contributions from both the NCs and the Ru complexes. However, at short times after excitation ($\Delta t < 5$ ns) the PL of the assembly is primarily due to the NCs. This conclusion can be made based on the fact that the instantaneous PL intensity measured during this time interval is greater for the mixture than for the reference Ru complex sample prepared with the same concentration of the complexes (compare traces shown by red circles and blue squares in Figure 5). The decay of NC PL in the assembly is significantly faster than that in the reference NC sample, indicating the existence of an additional high-efficiency relaxation channel that opens upon formation of NC complex assemblies. Further, we observe that the PL intensity in the mixture measured immediately after excitation is lower by approximately 80% than that for the NC reference sample although concentrations of the NCs in both samples are identical. This observation indicates that significant PL quenching in the assembly occurs on time scales that are shorter than the time resolution of the TCSPC experiment (40−50 ps).

One possible explanation for the observed quenching of the NC PL is that the NC surface passivation layer is disturbed in the presence of the complexes, which could potentially lead to enhanced surface trapping. However, this explanation is inconsistent with the observation that the PL of the Ru complexes is also quenched in the mixture as indicated by both steady-state (inset of Figure 5) and time-resolved (main frame of Figure 5) PL data. Specifically, at times longer than 10−20 ns after excitation the PL signal of the mixture is dominated by long-lived emission of the Ru complexes (corresponding lifetime is >300 ns). As evident from Figure 5, on these time scales the instantaneous PL intensity of the NC complex mixture is lower than that for the Ru complex reference, even though the concentration of the complexes is the same in both samples. The Ru complex PL quenching factor derived from time-resolved measurements ($I_{PL}(NC/Ru)/I_{PL}(Ru) \approx 0.5$ at $\Delta t = 75$ ns) is comparable to that calculated based on steady-state PL results (see above), providing additional confirmation that the formation of NC/Ru complex assemblies affects PL of both the NCs and the complexes.

The fact that emissions of the NC and the Ru complex are quenched simultaneously indicates strong electronic interactions between these species in the assembled structures. To determine the exact nature of these interactions, we performed femtosecond studies of carrier dynamics using TA and time-resolved PL upconversion (uPL) measurements.[33] The latter method is based on frequency mixing,[24] and its temporal resolution is determined by the duration of an optical gating pulse (~300 fs in our experiments).

In CdSe NCs, the TA dynamics recorded at the position of the 1S transition are primarily due to changes in the population of the 1S electron state. However, the PL intensity is determined by the product of the electron and hole occupation numbers.[21,22] Consequently, PL relaxation is dominated by hole dynamics if they are significantly faster than electron dynamics. (The latter is the case in the NC/$[Ru^{II}(bpy)(mcb)_2]^{2+}$ assemblies as indicated by results shown below.[21]) One can use this difference in origins of TA and PL signals to distinguish between electron and hole relaxation behaviors.[21]

Figure 6 displays TA and uPL time transients (collected at 600 and 615 nm, respectively) for the NC solution (A) and the NC/$[Ru^{II}(bpy)(mcb)_2]^{2+}$ assembly (B). In the case of the NC-only solution, uPL relaxation is slightly faster than TA relaxation, suggesting more efficient surface trapping of holes compared to electrons. While electron relaxation remains almost unchanged in the mixture (indicated by almost unchanged TA dynamics), the PL dynamics develop a short-lived, 5 ps component indicating fast depopulation of NC hole states. This result provides strong indication that NC PL quenching observed upon formation of NC/Ru complex assemblies is due to *hole transfer* from the photoexcited NCs to the surface-attached complexes (inset of Figure 6B). This process also quenches complex PL because the Ru(III) form of the complex is nonemissive.

The measured PL dynamics indicate a charge-transfer time of 5 ps, which is shorter than the characteristic Auger recombination times in NCs. This result suggests that the NC/$[Ru^{II}(bpy)(mcb)_2]^{2+}$-type assemblies can, in principle, be utilized for extraction of multiple redox equivalents produced in the NC via the CM process. This approach can potentially be used in the development of efficient photocatalysts by making use of the large absorption cross-sections of NCs, their broad, size-controlled absorption spectra, and their ability to produce multiple excitons per single absorbed photon.

4. Conclusions

We have shown that time-resolved PL is a useful tool for the study of CM. Through the use of this capability, the formation of multiple excitons within a NC following absorption of a single photon has been demonstrated both dynamically and, for the first time, spectrally. The dynamic method for the study of CM is remarkably similar to our previously demonstrated method based upon TA wherein dynamics associated with the presence of multiple excitons are differentiated from single-exciton dynamics. Time-resolved PL has also been shown to reveal CM spectrally. Specifically, we observe a red-shifted PL maximum at early time after photoexcitation, which is consistent with the presence of multiple excitons that experience attraction. We then presented experimental evidence that charge transfer from a CdSe NC to a surface-adsorbed Ru-based catalytic model compound takes place on a time scale that is faster than Auger recombination. This result suggests that the extraction ofmultiple charges from NCs following CM is feasible in such assemblies and demonstrates that opportunities exist for exploitation of the CM effect in practical applications, such as NC-assisted photocatalysis and photovoltaics.

Acknowledgment. This work was supported by the Chemical Sciences, Biosciences, and Geosciences Division of the Office of Basic Energy Sciences, Office of Science, U. S. Department of Energy and Los Alamos Laboratory Directed Research and Development funds. We thank Dr. J. Alstrum-Acevedo for providing Ru complex samples and Professor T. J. Meyer for helpful discussions.

References and Notes

(1) Koc, S. *Czech J. Phys. B* **1957**, *7*, 91.
(2) De Vos, A.; Desoete, B. *Sol. Energy Mater. Sol. Cells* **1998**, *51*, 413.
(3) Kolodinski, S.; Werner, J. H.; Wittchen, T.; Queisser, H. J. *Appl. Phys. Lett.* **1993**, *63*, 2405.
(4) Nozik, A. J. *Physica E* **2002**, *14*, 115.
(5) Werner, J. H.; Kolodinski, S.; Queisser, H. J. *Phys. Rev. Lett.* **1994**, *72*, 3851.
(6) Wolf, M.; Brendel, R.; Werner, J. H.; Queisser, H. J. *J. Appl. Phys.* **1998**, *83*, 4213.
(7) Schaller, R. D.; Klimov, V. I. *Phys. Rev. Lett.* **2004**, *92*, 186601.
(8) Schaller, R. D.; Petruska, M. A.; Klimov, V. I. *Appl. Phys. Lett.* **2005**, *87*, 253102/1.
(9) Schaller, R. D.; Klimov, V. I. *Phys. Rev. Lett.* **2006**, *96*, 097402.
(10) Schaller, R. D.; Sykora, M.; Pietryga, J. M.; Klimov, V. I. *Nano Lett.* **2006**, *6*, 424.
(11) Ellingson, R.; Beard, M. C.; Johnson, J. C.; Yu, P.; Micic, O. I.; Nozik, A. J.; Shabaev, A.; Efros, A. L. *Nano Lett.* **2005**, *5*, 865.
(12) Murphy, J. E.; Beard, M. C.; Norman, A. G.; Ahrenkiel, S. P.; Johnson, J. C.; Yu, P. R.; Micic, O. I.; Ellingson, R. J.; Nozik, A. J. *J. Am. Chem. Soc.* **2006**, *128*, 3241.
(13) Crooker, S. A.; Barrick, T.; Hollingsworth, J. A.; Klimov, V. I. *Appl. Phys. Lett.* **2003**, *82*, 2793.
(14) Du, H.; Chen, C.; Krishnan, R.; Krauss, T. D.; Harbold, J. M.; Wise, F. W.; Thomas, M. G.; Silcox, J. *Nano Lett.* **2002**, *2*, 1321.
(15) Wehrenberg, B. L.; Wang, C. J.; Guyot-Sionnest, P. *J. Phys. Chem. B* **2002**, *106*, 10634.
(16) Klimov, V. I.; Mikhailovsky, A. A.; McBranch, D. W.; Leatherdale, C. A.; Bawendi, M. G. *Science* **2000**, *287*, 1011.
(17) Schaller, R. D.; Petruska, M. A.; Klimov, V. I. *J. Phys. Chem. B* **2003**, *107*, 13765.
(18) Murray, C. B.; Norris, D. J.; Bawendi, M. G. *J. Am. Chem. Soc.* **1993**, *115*, 8706.
(19) Klimov, V. I. *J. Phys. Chem. B* **2000**, *104*, 6112.
(20) Achermann, M.; Hollingsworth, J. A.; Klimov, V. I. *Phys. Rev. B* **2003**, *68*, 245302.
(21) Klimov, V. I.; Schwartz, C. J.; McBranch, D. W.; Leatherdale, C. A.; Bawendi, M. G. *Phys. Rev. B* **1999**, *60*, R2177.
(22) Klimov, V. I.; McBranch, D. W.; Leatherdale, C. A.; Bawendi, M. G. *Phys. Rev. B* **1999**, *60*, 13740.
(23) Schaller, R. D.; Agranovich, V. M.; Klimov, V. I. *Nat. Phys.* **2005**, *1*, 189.
(24) Shah, J. *IEEE J. Quantum. Electron.* **1988**, *24*, 276.
(25) Xu, S.; Mikhailovsky, A. A.; Hollingsworth, J. A.; Klimov, V. I. *Phys. Rev. B* **2002**, *65*, 045319.
(26) Caruge, J. M.; Chan, Y.; Sundar, V.; Eisler, H. J.; Bawendi, M. G. *Phys. Rev. B* **2004**, *70*, 85316.
(27) Shionoya, H.; Saito, H.; Hanamura, E.; Akimoto, O. *Solid State Commun.* **1973**, *12*, 223.
(28) Greenham, N. C.; Peng, X.; Alivisatos, A. P. *Phys. Rev. B* **1996**, *54*, 17628.
(29) Logunov, S.; Green, T.; Marguet, S.; El-Sayed, M. A. *J. Phys. Chem. A* **1998**, *102*, 5652.
(30) Asbury, J. B.; Hao, E.; Wang, Y.; Ghosh, H. N.; Lian, T. *J. Phys. Chem. B* **2001**, *105*, 4545.
(31) Huynh, W. U.; Dittmer, J. J.; Alivisatos, A. P. *Science* **2002**, *295*, 2425.
(32) Robel, I.; Subramanian, V.; Kuno, M.; Kamat, P. V. *J. Am. Chem. Soc.* **2006**, *128*, 2385.
(33) Sykora, M.; Petruska, M. A.; Alstrum-Acevedo, J.; Bezel, I.; Meyer, T. J.; Klimov, V. I. *J. Am. Chem. Soc.* **2006**, *128*, 9984.